Available online at www.sciencedirect.com
ScienceDirect
Physics Letters A 358 (2006) 426–430
PHYSICS LETTERS A
www.elsevier.com/locate/pla

Curtain coating in microfluidics and the phenomenon of nonlocality in dynamic wetting

A.V. Lukyanov *, Y.D. Shikhmurzaev

School of Mathematics, University of Birmingham, Birmingham B15 2TT, UK

Received 21 April 2006; accepted 18 May 2006

Available online 30 May 2006

Communicated by V.M. Agranovich

Abstract

Curtain coating on a length scale typical of microfluidics is investigated theoretically in the framework of an earlier developed theory where dynamic wetting is treated as essentially a process of formation of a new liquid–solid interface. The results demonstrate that the actual dynamic contact angle between the free surface and the solid boundary depends not only on the wetting speed and material constants of the contacting media, as in the so-called 'slip models', but also on the flow field/geometry in the vicinity of the moving contact line. In other words, for the same wetting speed the dynamic contact angle can be varied by manipulating the flow conditions. This outcome is consistent with the conclusions drawn earlier from macroscopic experiments.

1. Introduction

One of the central issues in the physics of capillarity is the question of whether or not dynamic wetting, i.e. the process of spreading of a liquid over a solid surface, is a local phenomenon whose characteristics depend only on the speed at which the three-phase contact line moves across the solid substrate and the material parameters of the contacting media or is it nonlocal, i.e. dependent also on the flow field/geometry in the vicinity of the contact line. A flow configuration that offers sufficient flexibility to clarify this issue is the so-called 'curtain coating'. Curtain coating is a technique for depositing fluid films on solid surfaces in which a sheet of fluid impinges onto a moving solid substrate (Fig. 1). In addition to being one of the main coating methods in photographic and now paper industry [1], curtain coating is proven to be very useful for studying various features of dynamic wetting [2,3]. The main advantage of this flow configuration as an investigative tool is that, in addition to the wetting speed variations, it allows one to independently vary the flow rate, the curtain height and the angle between the falling sheet and the solid surface, thus making possible a multiparametric investigation into the role played by the overall flow field/geometry in the wetting process.

Recent experiments reported by Blake et al. [4] show that, for a given wetting speed, the measured contact angle between the free surface and the moving solid boundary depends on the flow field/geometry as it varies with the variation of the above parameters. A subsequent theoretical study [5] carried out in the framework of the so-called 'slip models', where, for a given solid/liquid/gas system, the actual contact angle θ_d (Fig. 1) is assumed to be a function of the wetting speed, has demonstrated that the observed effect cannot be explained in terms of the so-called 'apparent' contact angle (Fig. 1), i.e. by attributing it to free-surface bending in the immediate vicinity of the contact line. As was shown, the free-surface bending within the spatial resolution of the measurements (≈ 20 μm in [4]) is too small for the 'apparent' contact angle to account for the observed contact-angle variations. These findings lead to a fundamental conclusion that it is the actual contact angle, i.e. the angle at which the liquid–gas interface, described as a mathematical surface, meets the solid boundary, that varies with variations in the flow field.

* Corresponding author.
E-mail address: lukyanov@for.mat.bham.ac.uk (A.V. Lukyanov).

0375-9601/$ – see front matter
doi:10.1016/j.physleta.2006.05.048

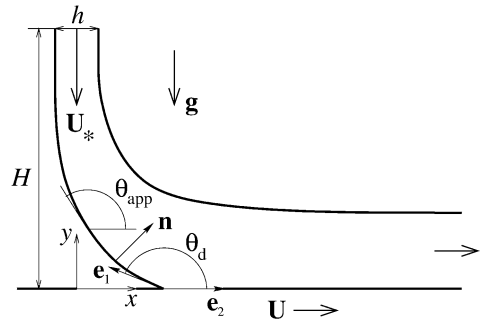

Fig. 1. Definition sketch for curtain coating. θ_d is the 'actual' contact angle, i.e. the angle at which the free surface meets a solid boundary in the macroscopic fluid mechanics modeling of the flow. θ_{app} is the so-called 'apparent' contact angle formed by the tangent to the free surface at some distance from the contact line and the solid substrate; this angle is often used as an auxiliary concept to interpret experimental data.

This effect is of particular importance in microfluidics where the length scale characterizing the flow geometry becomes comparable with the scale on which the specific physics of wetting that determines the dynamic contact angle operates. In the present work, we investigate the dependence of the dynamic contact angle on the flow field at low Reynolds numbers in the framework of an earlier developed theory [6], where dynamic wetting is treated as a particular case of a flow with forming/disappearing interfaces. In this theory, the length scale associated with the specific physics of wetting is the length over which the newly formed liquid–solid interface equilibrates. Then, generally speaking, one should expect nonlocality in the contact-angle behavior, i.e. its dependence on the flow geometry, when the length scale characterizing variations in the flow field becomes comparable with the equilibration length of the interfacial parameters. Importantly, in this theory the actual dynamic contact angle is not prescribed as a function of the contact-line speed and material constants of the system; instead, it is introduced via the (dynamic) Young equation (see (11) below) and hence has to be determined as part of the solution. The model based on this approach derived using methods of irreversible thermodynamics has been applied to analyze a number of experiments on dynamic wetting [6–8] as well as to some other flows where the formation/disappearance of interfaces takes place [9,10]. In the present work, we examine it from the viewpoint of the role played by the flow field and the physical mechanisms responsible for the contact angle behavior.

2. Problem formulation

The essence of the model to be used [6] is that, by its very definition, 'dynamic wetting' is the process of formation of a new 'wetted' solid surface, i.e. a fresh liquid–solid interface. Then the 'moving contact-line problem' can be seen as arising due to the fact that the process of interface formation is not accounted for in the standard fluid-mechanical formulation where all interfaces are treated as already formed. In [6], the problem is addressed by incorporating the process of formation/disappearance of the 'surface phase' into the boundary conditions for the Navier–Stokes equations that describe the bulk flow. To study dynamic wetting, generally as an unsteady process, in the framework of this model, one has to consider solutions of the Navier–Stokes equations,

$$\nabla\cdot\mathbf{u}=0,\qquad \rho(\partial\mathbf{u}/\partial t+\mathbf{u}\cdot\nabla\mathbf{u})=-\nabla p+\mu\nabla^2\mathbf{u}+\rho\mathbf{g}, \tag{1}$$

subject to the following boundary conditions. At an a priori unknown free surface $f(\mathbf{r},t)=0$ with the inward normal $\mathbf{n}=\nabla f/|\nabla f|$ the boundary conditions are given by:

$$\partial f/\partial t+\mathbf{v}^s\cdot\nabla f=0, \tag{2}$$

$$-p+\mu\mathbf{n}\cdot\left[\nabla\mathbf{u}+(\nabla\mathbf{u})^*\right]\cdot\mathbf{n}=\sigma\nabla\cdot\mathbf{n},$$

$$\mu\mathbf{n}\cdot\left[\nabla\mathbf{u}+(\nabla\mathbf{u})^*\right]\cdot(\mathbf{I}-\mathbf{nn})+\nabla\sigma=0, \tag{3}$$

$$\rho\left(\mathbf{u}-\mathbf{v}^s\right)\cdot\mathbf{n}=\left(\rho^s-\rho^s_{1e}\right)\tau^{-1},$$

$$\partial\rho^s/\partial t+\nabla\cdot\left(\rho^s\mathbf{v}^s\right)=-\left(\rho^s-\rho^s_{1e}\right)\tau^{-1}, \tag{4}$$

$$(1+4\alpha\beta)\nabla\sigma=4\beta\left(\mathbf{v}^s-\mathbf{u}\right)\cdot(\mathbf{I}-\mathbf{nn}), \tag{5}$$

whereas on the solid surface moving with velocity $\mathbf{U}$ one has:

$$\mu\mathbf{n}\cdot\left[\nabla\mathbf{u}+(\mathbf{u})^*\right]\cdot(\mathbf{I}-\mathbf{nn})+\frac{1}{2}\nabla\sigma=\beta(\mathbf{u}-\mathbf{U})\cdot(\mathbf{I}-\mathbf{nn}), \tag{6}$$

$$\rho\left(\mathbf{u}-\mathbf{v}^s\right)\cdot\mathbf{n}=\left(\rho^s-\rho^s_{2e}\right)\tau^{-1},$$

$$\partial\rho^s/\partial t+\nabla\cdot\left(\rho^s\mathbf{v}^s\right)=-\left(\rho^s-\rho^s_{2e}\right)\tau^{-1}, \tag{7}$$

$$\left(\mathbf{v}^s-\mathbf{U}\right)\cdot\mathbf{n}=0,\qquad \left[\mathbf{v}^s-\frac{1}{2}(\mathbf{u}+\mathbf{U})\right]\cdot(\mathbf{I}-\mathbf{nn})=\alpha\nabla\sigma. \tag{8}$$

Here $\mathbf{u}$ and p are the velocity and pressure (measured with respect to a constant pressure in the surrounding gas) in the liquid, whose density ρ and viscosity μ are assumed to be constant; $\mathbf{g}$ is the acceleration of gravity. On the free surface, in addition to the kinematic condition (2), which simply defines the normal component of velocity of the surface phase, and the usual conditions on the normal and tangential stresses (3), the model takes into account mass exchange between the bulk and the surface phase (4) as the surface density of the surface phase ρ^s relaxes to its equilibrium value ρ^s_{1e}. In (3) and (4), $\mathbf{I}$ is the metric tensor and τ is the relaxation time. Similar to (4), conditions (7) describe mass exchange between the bulk and the liquid–solid interface. Importantly, the tangential components of the velocity in the surface phase $\mathbf{v}^s$, the bulk velocity evaluated on the liquid-facing side of interfaces $\mathbf{u}$ and the velocity of the solid substrate $\mathbf{U}$ are, in a general case, different due to the torques acting on the surface phase. The conditions relating these components are given by (5) on the free surface and (6) and (8) on the solid boundary. It is assumed that the solid surface is impermeable for and inert with respect to the fluid (the first condition (8)) and there is no actual slip on the solid surface (hence the second condition (8) has the form of a 'Darcy law'). The equation of state in the surface phase that closes the set of equations (2)–(8) for the surface variables along the interfaces is taken in a simple 'barotropic' form linking the surface tension σ with the surface density:

$$\sigma=\gamma\left(\rho^s_{(0)}-\rho^s\right). \tag{9}$$

This equation is the simplest one accounting for the fact that the surface tension decreases from its equilibrium value $\sigma_{1e} = \sigma(\rho^s_{1e})$ in the free surface to that in the liquid–solid interface, $\sigma_{2e} = \sigma(\rho^s_{2e})$, when the interfacial layer becomes more compressed (or, more generally, less rarified) due to the action of intermolecular forces from the bulk phases that determine the equilibrium values of ρ^s. The dependence of phenomenological material constants α, β, γ and τ on viscosity and their estimates for particular fluids have been obtained by analyzing experiments on dynamic wetting available in the literature [7,8].

Distributions of the surface parameters along the interfaces are linked at the contact line via the mass and momentum balance conditions:

$$\rho^s_1\big(\mathbf{v}^s_1 - \mathbf{U}_{\rm cl}\big)\cdot\mathbf{e}_1 + \rho^s_2\big(\mathbf{v}^s_2 - \mathbf{U}_{\rm cl}\big)\cdot\mathbf{e}_2 = 0, \tag{10}$$

$$\sigma_1\cos\theta_d = \sigma_3 - \sigma_2, \tag{11}$$

where the subscripts 1 and 2 refer to the limiting values as one approaches the contact line along the free surface and the solid–liquid interface, respectively; $\mathbf{e}_1$ and $\mathbf{e}_2$ are unit normals to the contact line directed along the appropriate interfaces (Fig. 1); σ_3 is the tangential component of the reaction force acting on the contact line from the solid substrate; $\mathbf{U}_{\rm cl}$ is the velocity of the contact line. For the cosine of the dynamic contact angle θ_d one has $\cos\theta_d = \mathbf{e}_1\cdot\mathbf{e}_2$. In equilibrium, the dynamic contact angle is related to the static one, θ_s, via the classical Young equation

$$\sigma_{1e}\cos\theta_s = \sigma_3 - \sigma_{2e}$$

that links the material constants σ_{1e}, σ_{2e}, σ_3 (or, alternatively, after using (9), ρ^s_{1e}, ρ^s_{2e}, $\rho^s_{(0)}$, γ, σ_3) and hence allows one to replace one of them with θ_s, which is a quantity relatively easy to measure in experiments.

The boundary conditions (2)–(11) describe the surface phases and the contact line as elements of a fluid-mechanical model. For a steady curtain coating we drop $\partial/\partial t$ in (1), (2), (4), (7) and have to formulate additional boundary condition specifying this flow. After introducing a Cartesian coordinate system as shown in Fig. 1, one can set the inlet velocity and thickness of a falling liquid sheet:

$$\mathbf{u} = \mathbf{U}_* \quad \text{for } -h/2 \leqslant x \leqslant h/2,\ y = H,$$

where the inlet velocity $\mathbf{U}_*$ is assumed to have only the y-component. We will also assume that at the top of the curtain the interfaces are in equilibrium, i.e.

$$\rho^s = \rho^s_{1e}, \qquad \mathbf{v}^s = \mathbf{u} \quad \text{for } x = \pm h/2,\ y = H.$$

Finally, as the far downstream condition one can use soft boundary conditions for the bulk flow

$$\frac{\partial\mathbf{u}(x,y)}{\partial x} \to 0 \quad (x\to\infty,\ \forall y)$$

and the requirement that the interface tends to its equilibrium state

$$\rho^s \to \rho^s_{2e} \quad (x\to\infty,\ y = 0).$$

In a coordinate system where the contact line is at rest (Fig. 1), we obviously have $\mathbf{U}_{\rm cl} = 0$ in (10).

3. Numerical solution

Using U, h, $\mu U h^{-1}$, σ_{1e} and $\rho^s_{(0)}$ as scales for velocity, length, pressure, surface tension and the surface density, respectively, we have the problem whose solution is specified by the dimensionless similarity parameters that can be divided into the following three groups. First, it is the Reynolds and Froude numbers, $\mathrm{Re} = \rho U h/\mu$, $\mathrm{Fr} = U^2/(gh)$, i.e. the parameters that characterize the bulk flow. In microfluidics, one almost invariably has creeping flows with negligible inertia. For the problem we are considering $h \sim 2$–4 μm, $U \sim 1\ \mathrm{cm\,s^{-1}}$, $\mu/\rho \sim 60$ cSt giving $\mathrm{Re} \leqslant 10^{-3}$, so that the convective term in (1) can be neglected. Although the ratio Re/Fr is also small ($\leqslant 4\times 10^{-4}$ for our flow conditions), in the computations we will keep the body force term in (1) as the stabilizing factor for the film far downstream the solid substrate.

The second group of dimensionless coefficients includes, firstly, the similarity parameters formed by the material constants characterizing the contacting media, θ_s, $\bar\rho^s_{1e} = \rho^s_{1e}/\rho^s_{(0)}$, $A = \alpha\beta$, $\bar\sigma_3 = \sigma_3/\sigma_{1e}$, and, secondly, the parameters depending on material constants and the contact-line speed only: $\mathrm{Ca} = \mu U/\sigma_{1e}$, $Q = \rho^s_{(0)}/(\rho U\tau)$, $\bar\beta = \beta U h/\sigma_{1e}$ and $\epsilon = U\tau/h$. All these parameters remain fixed for a given set of materials and a given contact-line speed.

Finally, we have two parameters, $\bar U_* = U_*/U$, $\bar H = H/h$, whose variation, for a given contact-line speed, leads to variation in the flow field/geometry in the vicinity of the contact line. We will consider the role played by $\bar U_*$. This analysis will help to understand the mechanism of the effect that came to be known as 'hydrodynamic assist of dynamic wetting' [2].

The problem was solved numerically using a combined BIE-FE algorithm that has the capacity to resolve the distributions of the surface parameters in the immediate vicinity of the contact line and handle the contact angle itself with sufficient accuracy (the finite element part of the method) and at the same time allows one to describe the creeping free-surface flow away from the contact line in an efficient and flexible way (the boundary integral equation part). The details of the algorithm can be found elsewhere [11].

The main difficulty in computing the solution arises due to the physical effect we are trying to capture. The formulation (1)–(11) introduces the dynamic contact angle via the Young equation (11) and hence makes it part of the solution dependent on the dynamic values of the surface tensions at the contact line, which in their turn are determined by the distributions of the surface parameters along the interfaces. These distributions are linked with the bulk stress and velocity evaluated at the interfaces thus making θ_d a functional of the flow field. On the other hand, however, the value of θ_d is a boundary condition for the equation specifying the shape of the flow domain, thus giving a feedback to the flow field. This interdependence of the bulk, interfacial and contact-line characteristics makes even a numerical solution of the problem (1)–(11) difficult to obtain since, in addition to the known difficulties of computing free-boundary flows [12], one has to pay particular attention to the accuracy with which the distributions of the surface parameters along the interfaces are resolved. It is their values at the

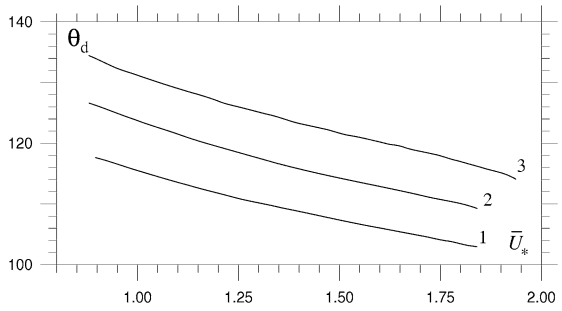

Fig. 2. Dependence of the dynamic contact angle on the dimensionless inlet velocity for $\bar{H} = 10$ and different contact-line speeds. 1: Ca $= 0.02$, $Q = 0.041$, $\bar{\beta} = 20$, $\epsilon = 0.0245$. Curves 2 and 3 are obtained by increasing the contact-line speed by 12.5 and 25%, respectively; $\theta_s = 60°$, $\bar{\rho}^s_{1e} = 0.8$, $A = 1$, $\bar{\sigma}_3 = 0$ for all curves.

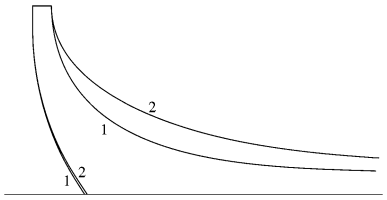

Fig. 3. Typical profiles of the curtain. The two profiles are obtained for essentially different contact-line speeds (1: Ca $= 0.0225$; 2: Ca $= 0.025$; other dimensionless parameters scaled with U change accordingly) and have approximately the same contact angle ($\approx 120°$) due to manipulating the flow conditions (1: $\bar{U}_* = 1.15$; 2: $\bar{U}_* = 1.58$). In the horizontal direction, the plot is clipped at approximately 0.15 of the actual size of the computational domain.

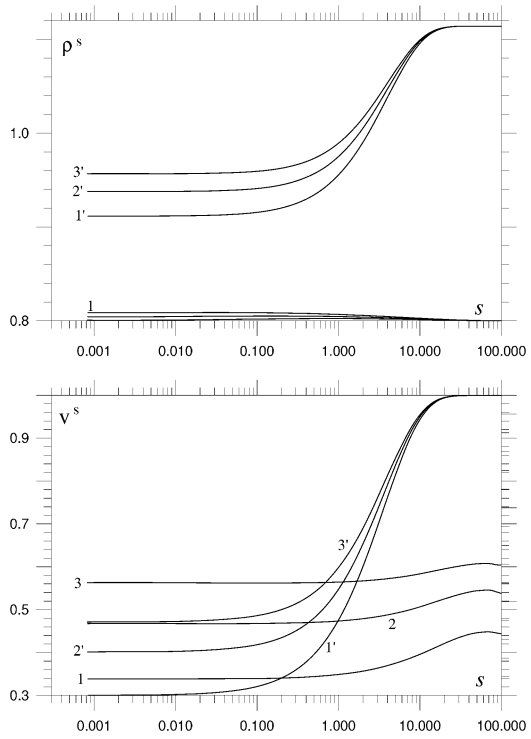

Fig. 4. Distributions of the surface parameters along the free surface and the liquid–solid interface (marked with a prime) at different points along curve 1 of Fig. 2. 1: $\bar{U}_* = 0.91$, 2: $\bar{U}_* = 1.38$, 3: $\bar{U}_* = 1.82$. The distance s from the contact line is scaled with $U\tau$; the data point corresponding to $s = 0$ is taken out.

contact line that, via the contact angle, have a global effect on the shape of the computational domain, hence on the bulk flow, which in its turn affects the surface distributions. As a result, every element of the model turns out to be sensitive to the accuracy with which all other elements are computed, and the control of computational accuracy becomes a formidable task.

The effect of the inlet velocity $\bar{U}_*$ on the dynamic contact angle is summarized in Fig. 2. As one can see, for a given value of U the dynamic contact angle can indeed be varied by varying the flow field: θ_d decreases as U_* goes up. An alternative way of interpreting Fig. 2 is that it shows that the dependence of θ_d on the capillary number (i.e. dimensionless contact-line speed) is different for different flow fields/geometries, which in our case are specified by $\bar{U}_*$ and $\bar{H}$. This nonuniqueness of the velocity-dependence of the dynamic contact angle was indeed observed in experiments [4] (for macroscopic curtains at finite Reynolds numbers so that a direct comparison with our computations is not possible).

The possibility of having the same dynamic contact angle at different contact-line speeds by manipulating the flow conditions is illustrated in Fig. 3. It is important to emphasize that, as our calculations demonstrate, the theory predicts no drastic variations of the free-surface slope in the immediate vicinity of the contact line and hence, for the spatial resolution of standard optical techniques, the measured (or 'apparent') contact angle can be taken as a reasonably accurate representation of the actual one.

As we mention earlier, all elements in the model are interdependent and therefore, strictly speaking, it would be incorrect to single out direct causal links between any two of them in terms of 'causes' and 'consequences'. However, for relatively low capillary numbers in the flow we are considering here one can arrive at a qualitative understanding of the mechanism by which the flow field influences the dynamic contact angle after examining the distributions of the surface variables ρ^s and v^s corresponding to different points along one of the curves given in Fig. 2. These distributions are shown in Fig. 4.

As the distributions of the surface density show (Fig. 4), the deviation of ρ^s on the free surface from its equilibrium value, being proportional to Ca, is small and hence the mass flux into the contact line that features in (10) is determined primarily by the value of v^s there. This value increases as the inlet velocity $\bar{U}_*$ goes up, thus increasing the mass flux into the forming liquid–solid interface. In the process of dynamic wetting, the liquid–solid interface near the contact line is generally 'starving' since it begins to form out of the liquid–gas interface that moves into the contact line with the velocity lower than the velocity of the solid substrate that drags the (solid-facing side of the) liquid–solid interface out of the contact line and has a lower equilibrium surface density than that of the liquid–solid interface. Therefore, an increase in v^s on the free surface due to an increase in $\bar{U}_*$ reduces 'starvation' of the liquid–solid interface, i.e. the difference between its surface density at the contact line and far away from it (Fig. 4). Then, according to the Young equation (11), this leads to a decrease in the value of the dy-

namic contact angle which acts as a mechanism balancing the tangential forces acting on the contact line. In other words, an increase in the mass flux into the contact line from the free surface brings the surface density of the liquid–solid interface at the contact line closer to its equilibrium value and hence drives θ_d closer to θ_s.

Thus, for small capillary numbers the mechanism of the influence of the flow field on the dynamic contact angle is relatively transparent: the contact angle responds to the influence of the flow conditions on the tangential velocity of the free surface near the contact line that controls the supply of mass for the formation of the liquid–solid interface. An increase in v^s reduces 'starvation' of the liquid–solid interface and hence the contact angle, thus, using the terminology of [2], 'assisting' dynamic wetting.

A key requirement for the above 'hydrodynamic assist' to take place is that the length scale characterizing variations in the flow field must be comparable with the surface-tension-relaxation length. In our model, this condition is reflected in the parameter ϵ which is exactly the ratio of the two lengths. Computations show that, if the system as a whole is magnified (i.e. h and H proportionally increase), the effect of 'hydrodynamic assist' eventually disappears. (Formally, for a given system, the magnitude of the effect can be attributed to one parameter, ϵ, by eliminating h from $\bar{\beta}$, i.e. replacing it with $\epsilon\bar{\beta}$. This parameter would then be proportional to V^2 introduced in [6].)

A material-related factor that determines the magnitude of the effect of 'hydrodynamic assist' is $1 - \bar{\rho}^s_{1e} = \sigma_{1e}/(\gamma\rho^s_{(0)})$, which is essentially a measure of rarefaction of the interfacial layer. The closer $\bar{\rho}^s_{1e}$ is to 1, the smaller is the possible amplitude of variation of the surface density, $\bar{\rho}^s_{2e} - \bar{\rho}^s_{1e}$, and hence the stronger becomes the influence of changes in v^s that result in variations of θ_d. This sensitivity of θ_d to $1 - \bar{\rho}^s_{1e}$ (i.e. to $\sigma_{1e}/(\gamma\rho^s_{(0)})$) could be used in experiments to investigate the equation of state in the surface phase.

4. Conclusion

It has been shown that the theory of dynamic wetting as an interface formation process predicts that, for a given contact-line speed and materials of the system, the actual dynamic contact angle θ_d depends on the flow field/geometry in the vicinity of the moving contact line. This effect becomes more pronounced as the ratio of the surface-tension-relaxation length $U\tau$ to the length scale characterizing variations in the (Stokes) flow near the contact line due to changes in the flow conditions increases. In the case of small (though finite) capillary numbers, the mechanism of the dependence of the dynamic contact angle on the flow field can be explained in terms of the latter's influence on the tangential velocity of the free surface that determines the mass flux into the contact line that goes into the formation of a fresh liquid–solid interface. The magnitude of response of the contact angle to the changes in the flow field depends on the material constants specifying the equation of state in the surface phase.

References

[1] S.F. Kistler, P.M. Schweizer (Eds.), Liquid Film Coating, Chapman & Hall, London, 1997.
[2] T.D. Blake, A. Clarke, K.J. Ruschak, AIChE J. 40 (1994) 229.
[3] A. Clarke, Chem. Eng. Sci. 50 (1995) 2397.
[4] T.D. Blake, M. Bracke, Y.D. Shikhmurzaev, Phys. Fluids 11 (1999) 1995.
[5] M.C.T. Wilson, J.L. Summers, Y.D. Shikhmurzaev, A. Clarke, T.D. Blake, Phys. Rev. E 73 (2006) 041606.
[6] Y.D. Shikhmurzaev, Int. J. Multiphase Flow 19 (1993) 589.
[7] Y.D. Shikhmurzaev, Phys. Fluids 9 (1997) 266.
[8] T.D. Blake, Y.D. Shikhmurzaev, J. Colloid Interface Sci. 253 (2002) 196.
[9] Y.D. Shikhmurzaev, Phys. Lett. A 245 (2005) 378.
[10] Y.D. Shikhmurzaev, IMA J. Appl. Math. 70 (2005) 880.
[11] A.V. Lukyanov, Y.D. Shikhmurzaev, J. Comput. Phys., 2006, submitted for publication.
[12] W.-T. Tsai, D.K.P. Yue, Annu. Rev. 28 (1996) 249.